Available online at www.sciencedirect.com

ScienceDirect

Proceedings of the Combustion Institute 36 (2017) 2025–2032

Proceedings of the Combustion Institute

www.elsevier.com/locate/proci

Parallel on-the-fly adaptive kinetics in direct numerical simulation of turbulent premixed flame

Suo Yang, Reetesh Ranjan, Vigor Yang, Suresh Menon, Wenting Sun*

School of Aerospace Engineering, Georgia Institute of Technology, Atlanta, GA 30332, USA

Received 3 December 2015; accepted 6 July 2016
Available online 18 July 2016

Abstract

A new numerical framework for direct numerical simulation (DNS) of turbulent combustion is developed employing on-the-fly adaptive kinetics (OAK), correlated transport (CoTran), and a point-implicit ODE solver (ODEPIM). The new framework is tested on a canonical turbulent premixed flame employing a real conventional jet fuel mechanism. The results show that the new framework provides a significant speed-up of kinetics and transport computation, which allows DNS with large kinetic mechanisms, and at the same time maintains high accuracy and good parallel scalability. Detailed diagnostics show that calculation of the chemical source term with ODEPIM is 17 times faster than with a pure implicit solver in this test. OAK utilizes a path flux analysis (PFA) method to reduce the large kinetic mechanism to a smaller size for each location and time step, and it can further speed up the chemical source calculation by 2.7 times in this test. CoTran uses a similar correlation method to make the calculation of mixture-averaged diffusion (MAD) coefficients 72 times faster in this test. Compared to conventional DNS, the total CPU time of the final framework is 20 times faster, kinetics is 46 times faster, and transport is 72 times faster in this test.

Keywords: Turbulent flames; Direct numerical simulation; Reaction kinetics

1. Introduction

The development of advanced combustion energy conversion systems requires accurate simulation tools, such as Direct Numerical Simulation (DNS) and Large Eddy Simulation (LES), for ignition, combustion instability, lean blow-out, and emissions. Because of high computational cost, DNS and LES typically employ simplified kinetic mechanisms. Oversimplified kinetic mechanisms, however, are known to be of limited functions and may significantly reduce the quality of prediction [1]. Detailed kinetic mechanisms must be considered for accurate prediction, which normally contain a large number of species. In combustion systems, the characteristic timescales can range from millisecond to picosecond or even beyond, so it is prohibitive to use detailed kinetic mechanisms in DNS/LES of turbulent combustion with a large number of grid cells. As a result, chemistry and transport dominate the resource requirements in most combustion DNS studies [2–5].

* Corresponding author.
E-mail address: wenting.sun@aerospace.gatech.edu (W. Sun).

http://dx.doi.org/10.1016/j.proci.2016.07.021
1540-7489 © 2016 by The Combustion Institute. Published by Elsevier Inc.

In order to reduce the number of species in detailed kinetic mechanisms, several methods [6–8] have been proposed. While the globally reduced kinetic mechanisms of around 40 species are small enough for most 0D/1D simulations, they are still too large for 3D simulations of turbulent combustion. On the other hand, any further reduction would introduce significant errors, because globally reduced mechanisms typically have to be produced based on conditions of interest in practice. To deal with this issue, several adaptive combustion models have been proposed by a number of investigators. Gou et al. [9] proposed a dynamic adaptive chemistry method with error control for 0D/1D laminar flames, reducing kinetics locally for each grid point and time step. Liang et al. [10] proposed a pre-partitioned adaptive chemistry methodology for 0D partially-stirred reactor using particle probability density function (PDF) methods. In contrast, Wu et al. [11] designed a sub-model assignment framework to assign different flamelet/finite rate sub-models rather than different kinetics to different zones of the simulation domain for a 2D laminar triple flame. This method matches the boundaries of zones by only conserving the interested quantities. Both the on-the-fly reduction and zone partition in all the above methods contain significant CPU overhead for mechanism reduction/zone partition. In order to reduce the CPU overhead, Liang et al. [10] and Wu et al. [11] proposed pre-generating look-up tables for the zone partition. Covering all conditions through tabulation, however, presents challenges, and the large tables make important demands on memory resources. Recently, Sun et al. [12,13] proposed a simple zone-partition criterion to decide whether a new on-the-fly reduction was required or not, and this significantly reduced CPU overhead. Employing the on-the-fly adaptive kinetics (OAK) technique, Sun et al. [12,13] showed significant reduction of CPU time for chemistry in 1D laminar flames.

Molecular diffusion transport modeling is another obstacle to accurate and efficient DNS of turbulent combustion. Bruno et al. [2] compared three models in DNS of a partially premixed flame, and concluded that the mixture-averaged diffusion (MAD) model predicts essentially the same fluid-dynamic and thermo-chemical field as the fully multi-component diffusion (MCD) model, but the fast constant Lewis number model predicts a significantly different flow field. Therefore, the MAD, or a higher fidelity, model is needed to guarantee accurate predictions. Although much faster than the MCD model, applying the MAD model at every time step and every grid cell is still expensive; it is often the 2nd largest component of the CPU time for a given computation, and could dominate CPU use if the kinetic source term is accelerated. To improve the computation of transport properties, Sun and Ju [14] developed a correlated transport (CoTran) technique, and obtained significant further speed-up for extensive 0D/1D laminar flames.

Both the OAK and CoTran techniques have been applied only to 0D and 1D simulations of laminar flames. Generalization of these techniques to 3D DNS of turbulent combustion gives rise to several critical questions: (1) how to efficiently scan and form the correlation zones in 3D space; (2) whether existing CPU overhead reduction methods are adequate for 3D turbulent flames; (3) whether correlation grouping is valid under high intensity turbulence; (4) how to maintain good parallel scaling performance on a large number of processors. In addition, optimized combinations of the above methods to provide the best possible speed have not yet been developed.

In the present work, a new regime-independent framework for 3D DNS of turbulent combustion with detailed kinetics is developed by incorporating on-the-fly adaptive kinetics (OAK), correlated transport (CoTran) techniques, and an efficient point-implicit ODE solver (ODEPIM) into a conventional DNS platform. All three methods are modified and optimized to adapt to 3D turbulent combustion and parallel high performance computing (HPC). The new framework is tested on a canonical premixed flame interacting with decaying isotropic turbulence to evaluate its accuracy, speed-up and parallel performance.

2. Numerical methods

2.1. Reacting flow solver

A well-established numerical flow solver, AVF-LESLIE [15], is employed in this study. It is a multi-physics simulation tool capable of DNS/LES of reacting/non-reacting flows in canonical and moderately complex flow configurations. It has been extensively used in the past to study wide variety of flow conditions, including acoustic flame-vortex interaction, premixed flame turbulence interaction, and scalar mixing [15,16]. It solves the reactive, multi-species, compressible Navier–Stokes equations using a finite-volume-based spatial discretization on generalized curvilinear coordinates. The spatial discretization is based on the well-known 2nd/4th-order accurate MacCormack scheme [17]. The time integration of the semi-discrete system of equations is performed by an explicit 2nd-order accurate scheme. The solver can handle arbitrarily complex finite-rate chemical kinetics and uses double-precision variable-coefficient stiff ODE solver (DVODE) [18]. The thermodynamic properties are computed using a thermally perfect gas formulation, whereas transport properties are obtained through MAD expressions.

2.2. Point-implicit ODE solver

ODEPIM [19,20] is a semi-implicit stiff ODE solver, which is more efficient than pure implicit ODE solvers due to its pointwise decoupling inside its inner iteration. For the same reason, its accuracy should be between that of pure explicit solvers, such as 4th-order Runge–Kutta (RK4), and that of pure implicit solvers, such as DVODE. Past studies [19,20] show that its accuracy is close to that of DVODE and its speed is close to that of RK4.

2.3. On-the-fly adaptive kinetics

The kernel engine of OAK is a path flux analysis (PFA) method [8] for kinetic mechanism reduction. The PFA method can select important species and reactions based on both production and destruction fluxes. The PFA reduction procedure begins with a list of preselected important species, typically fuel, and oxygen, and then selects all species with significant correlation to the selected species to form a sub-mechanism.

The basic idea of OAK is to generate reduced kinetics for each spatial location and time step (via the PFA method). To guarantee conservation of species, transport equations of inactive species are still solved but their chemical source terms are frozen to zero. Unfortunately, doing on-the-fly reduction by simply applying the PFA method for each grid cell and time step demands significant CPU overhead, which severely reduces the benefits of OAK [9]. In fact, many spatial locations and time steps have similar thermo-chemical states, thus could share the same reduced kinetics. For this reason, the PFA calculation is required for only one point in each space-time zone of similar thermo-chemical state, and other points can copy and use the same reduced kinetics decreasing the CPU overhead requirements [12,13]. During the calculation, OAK scans all grid cells in dictionary order. Adjacent time steps and spatial neighbors are likely to correlate to each other. Therefore, the correlation checking procedure is conducted on a 7-point stencil (center, upper, lower, front, back, left, and right) for each 3D grid cell. In particular, OAK checks the time correlation first by comparing the thermo-chemical states between the present and previous time steps at this grid cell. If they are correlated according to a pre-specified criterion, then the reduced kinetics on this grid cell do not need to change. Otherwise, OAK will check the 3D space correlation by comparing the thermo-chemical state of the present grid cell with the most updated states of its 6 neighbors. If any one of them is correlated to the present grid cell, then its most updated reduced kinetics will be copied and used for the present grid cell. Otherwise a new locally reduced mechanism must be generated. As the time advances, less and less new reduction is required due to the increase of space and time correlations. It is noteworthy that the performance of OAK is independent of ODE solver.

The key for time and space correlation is a reasonable pre-specified criterion. In order to form a suitable criterion, important marker species and thermodynamic state variables need to be selected. According to equivalence ratio effects and the Arrhenius law, fuel, O_2, and temperature should be considered in this criterion. Radicals and intermediate species are critical for combustion. In this study, OH is selected as the marker of high temperature chemistry and CH_2O and HO_2 are included in the criterion because they are marker species for low temperature chemistry [13]. The resulting criterion is the following (quantities with superscript 'o' represent the values at candidate time step/grid cell):

$$\Delta = \left(\frac{|T - T^o|}{\epsilon_T}, \frac{|\log Y_{fuel} - \log Y^o_{fuel}|}{\epsilon_Y}, \frac{|\log Y_{ox} - \log Y^o_{ox}|}{\epsilon_Y}, \frac{|\log Y_{\mathrm{OH}} - \log Y^o_{\mathrm{OH}}|}{\epsilon_Y}, \frac{|\log Y_{\mathrm{CH_2O}} - \log Y^o_{\mathrm{CH_2O}}|}{\epsilon_Y}, \frac{|\log Y_{\mathrm{HO_2}} - \log Y^o_{\mathrm{HO_2}}|}{\epsilon_Y} \right) \tag{1}$$

When $\|\Delta\|_\infty \le 1$, the two states are considered as correlated to each other, and can share the same reduced kinetic mechanisms. The thresholds are set as $\epsilon_T = 20\,\mathrm{K}$ and $\epsilon_Y = 25\%$. Past work shows that the accuracy of OAK is not sensitive to these thresholds [13]. When the concentration of a species is too small, large relative uncertainty arises. Therefore any of the above five species with a very small mass fraction ($< 10^{-6}$) should be removed from the criterion to avoid unnecessary reduction.

2.4. Correlated transport

In conventional simulations, transport properties based on the MAD model are computed at every time step and grid point, and this takes a significant amount of CPU time. Diffusion coefficients, in fact, also contain time and space correlations. For instance, the unburnt/burnt regions far from the premixed flame should have similar transport properties. In the quasi-steady state, the diffusion coefficients from one time step to the next change only slightly. Therefore, only one time computation is needed in each space-time correlation zone for transport properties, and the calculated diffusion coefficients are copied to every point in the zone [14]. Again, the copy operations are confined within each processor to eliminate MPI communication, and a 7-point stencil is adopted for time and space correlation checking. Unlike OAK, CoTran has no CPU overhead except for the correlation checking, so it is highly efficient. The performance of CoTran is also independent of ODE solver.

The primary difference between CoTran and the correlation grouping in OAK is the selection of marker parameters in the correlation criterion, which should reasonably represent the transport properties rather than kinetic reactivity. In most models [21], viscosity μ_k and conductivity k_k of the pure kth species depend only on temperature, whereas mass diffusivity D_k depends on both temperature and pressure, but ρD_k only depends on temperature. Therefore, temperature must be considered in the criterion while the pressure need not be, if ρD_{mix} rather than D_{mix} is calculated and copied during CoTran. Based on the Wilke formula [22] of the MAD model, diffusion coefficients of gas mixture are nonlinear combinations of those of pure species weighted by their concentrations. Therefore, species with larger concentration make a greater contribution to the transport properties of the gas mixture, even if they are inertial. In this study, fuel, O_2, N_2, CO, CO_2, H_2, and H_2O contribute more than 95% of the total concentration. The resulting criterion is the following [14]:

$$dist = \left(\frac{T - T^o}{T^o}, \frac{Y_{N_2} - Y^o_{N_2}}{Y^o_{N_2}}, \frac{Y_{fuel} - Y^o_{fuel}}{Y^o_{fuel}}, \frac{Y_{O_2} - Y^o_{O_2}}{Y^o_{O_2}}, \frac{Y_{H_2} - Y^o_{H_2}}{Y^o_{H_2}}, \frac{Y_{H_2O} - Y^o_{H_2O}}{Y^o_{H_2O}}, \frac{Y_{CO} - Y^o_{CO}}{Y^o_{CO}}, \frac{Y_{CO_2} - Y^o_{CO_2}}{Y^o_{CO_2}} \right) \quad (2)$$

When $\|dist\|_\infty \leq \epsilon_{tran}$, the CoTran threshold, the two states are considered as correlated to each other with respect to transport properties, and their transport properties are taken to be equal. In this study ϵ_{tran} is 5%, which is larger than the contribution from species other than the above seven.

3. Results and discussion

The kinetic mechanism used in this study is a real jet fuel pyrolysis mechanism ($C_{11}H_{22}$, Hai Wang, Stanford University, personal communication, 2015). The detailed kinetic mechanism contains 112 species and 790 elementary reactions, and so is prohibitively large for use in DNS. For validation purposes, therefore, a globally reduced kinetic mechanism from this detailed kinetic mechanism is used instead. The globally reduced kinetic model (Y. Gao, T. Lu, R. Xu, H. Wang, D.F. Davidson, C.T. Bowman, R.K. Hanson, personal communication, 2015) contains 38 species and 185 elementary reactions, and has been extensively validated against the detailed kinetic mechanism for parameters such as flame speed, ignition delay, and blowout.

A canonical turbulent premixed flame configuration corresponding to the thin reaction-zone regime based on the initial conditions ($\frac{u'}{S_L} = 15$, $\frac{l}{\delta_f} = 0.87$, where u' is the root-mean-square velocity fluctuations, S_L is the flame speed, l is the integral length-scale, and δ_f is the thermal flame thickness) is considered, where an initially planar premixed flame front interacts with a decaying isotropic turbulence. The computational domain consists of a cube with length 0.015 m. Periodic boundary conditions are specified in the spanwise (z) and transverse (y) directions, whereas a characteristic based inflow/outflow boundary condition [23] is specified in the x-direction with a mean flow velocity of 1.5 m/s. The initial isotropic turbulence is generated following the Kraichnan spectrum [24] and the planar flame solution is obtained at equivalence ratio of 0.8 (unburnt temperature is 300 K, and pressure is 1 atm). All the simulations are conducted to 1.5 times initial eddy turn-over time (0.127 ms) to allow flame-turbulence interactions to evolve.

3.1. Verification

To verify the new DNS framework proposed in this study, simulation results from the conventional DNS with the DVODE solver and the new DNS framework integrating ODEPIM, OAK, and CoTran methods are compared at the end of the simulation time. Full scale DNS simulations with grid size smaller than the Kolmogorov length-scales and large kinetic mechanism is prohibitive for conventional DNS with DVODE solver, so the verification is conducted on a coarse grid of 64^3 cells ($\frac{\delta_f}{\Delta x} = 1.8$, $k_{max}\eta = 0.178$, where k_{max} is the grid wavenumber, and η is the Kolmogorov length-scale). Therefore, the results presented here should be considered as coarse DNS. Note that ODEPIM + OAK + CoTran has run on a fine grid of 384^3 grid cells ($\frac{\delta_f}{\Delta x} = 11$, $k_{max}\eta = 1.069$) using 1728 processors and finished 1.5 initial eddy turn-over time within 86,400 total CPU hours.

Figure 1 shows a comparison of temperature and vorticity from the two methods. Both methods capture the same wrinkled flame as shown by temperature field and density field. Due to gas expansion, turbulence is damped on the products side. This phenomenon is captured by both methods as shown by the vorticity field. Therefore, the new framework well-reproduces results for thermodynamic state and flow field.

It is important to verify that the locally reduced kinetics from OAK can provide accurate reaction rates and concentrations. Fuel mass fraction and reaction rate for the two methods are shown in Fig. 2. Wrinkling of the flame surface can be observed in both quantities, but the flame remains contiguous while the reaction rate contour is disconnected, due to turbulence fluctuations. For both mass fraction and reaction rate, there is no observable difference between the two methods.

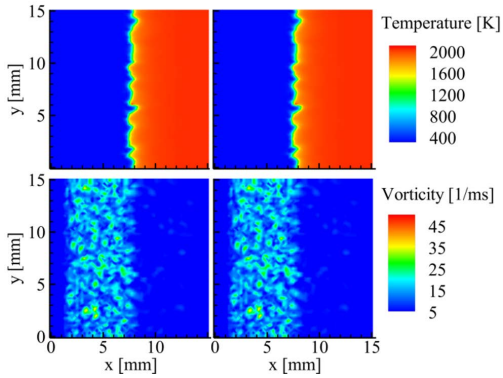

Fig. 1. Temperature (upper) and vorticity (lower) at the center plane ($z = 0.75$ cm) using conventional DNS (left) and proposed framework (right).

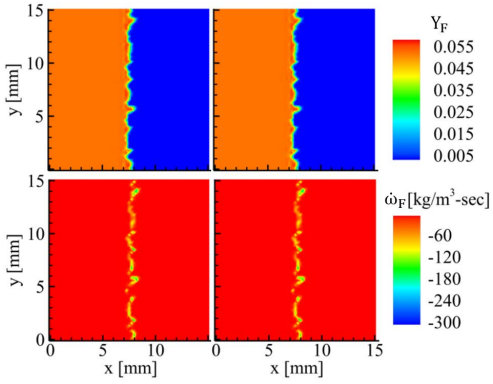

Fig. 2. Mass fraction (upper) and reaction rate (lower) of fuel at the center plane ($z = 0.75$ cm) from conventional DNS (left) and proposed framework (right).

Since there is no observable difference between the two methods based on 2D contours, more quantitative comparison is conducted to further evaluate the accuracy of the new frameworks. In Fig. 3, streamwise profiles of the spatially-averaged flame structure of the conventional DNS with DVODE solver and three new frameworks ODEPIM, ODEPIM + OAK, ODEPIM + OAK + CoTran are compared, and show no observable difference. Based on the fuel mass fraction profile in Fig. 3, unburned mixture, reaction region, and burned mixture account for 46.76%, 19.36%, and 33.88% of the computational domain, respectively.

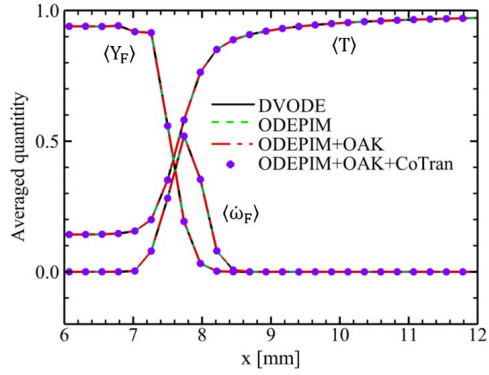

Fig. 3. Streamwise profiles of spatially-averaged scaled temperature, fuel mass fraction, and fuel reaction.

In Fig. 4, PDF profiles of mass fractions and reaction rates are compared among the conventional DNS with DVODE solver and three new frameworks. The complete PDF profiles show almost no difference among the four methods, so all profiles are zoomed in to show detailed differences.

To further quantify the errors introduced by the new methods, L_2 and L_∞ errors are calculated using the conventional DNS with DVODE solver as the benchmark case. Table 1 shows both L_2 and L_∞ errors of the three new frameworks. All L_2 errors are very small, and increase slightly from ODEPIM to ODEPIM + OAK to ODEPIM + OAK + CoTran. L_∞ errors show some rare but extreme behaviors of the new methods concealed by L_2 errors. As expected, L_∞ errors are significantly larger than the corresponding L_2 errors. From ODEPIM to ODEPIM + OAK to ODEPIM + OAK + CoTran, L_∞ errors are not monotonically increasing, and even decrease for temperature, Y_{OH}, and $\dot{\omega}_F$. Relative errors of ODEPIM + OAK + CoTran at mean flame plane ($x = 0.75$ cm) is shown in Fig. S1 in the Supplemental material. Relative errors of temperature are always smaller than 0.5%. All locations

Table 1
L_2 and L_∞ errors of the three frameworks.

Error	Temperature (K)	Y_F	Y_{OH}	$\dot{\omega}_F$ [$\frac{kg}{m^3 \cdot sec}$]	$\dot{\omega}_{OH}$ [$\frac{kg}{m^3 \cdot sec}$]
ODEPIM (L_2)	1.19E−4	5.91E−09	9.50E−10	1.30E−4	1.01E−05
ODEPIM + OAK (L_2)	1.27E−4	6.46E−09	1.09E−09	1.36E−4	2.77E−05
ODEPIM + OAK + CoTran (L_2)	3.52E−4	1.02E−08	1.59E−09	1.62E−4	2.85E−05
ODEPIM (L_∞)	9.83	1.80E−04	7.89E−05	12.83	7.22E−01
ODEPIM + OAK (L_∞)	9.74	1.92E−04	7.75E−05	12.83	1.05E+00
ODEPIM + OAK + CoTran (L_∞)	9.36	2.28E−04	7.44E−05	12.38	1.09E+00

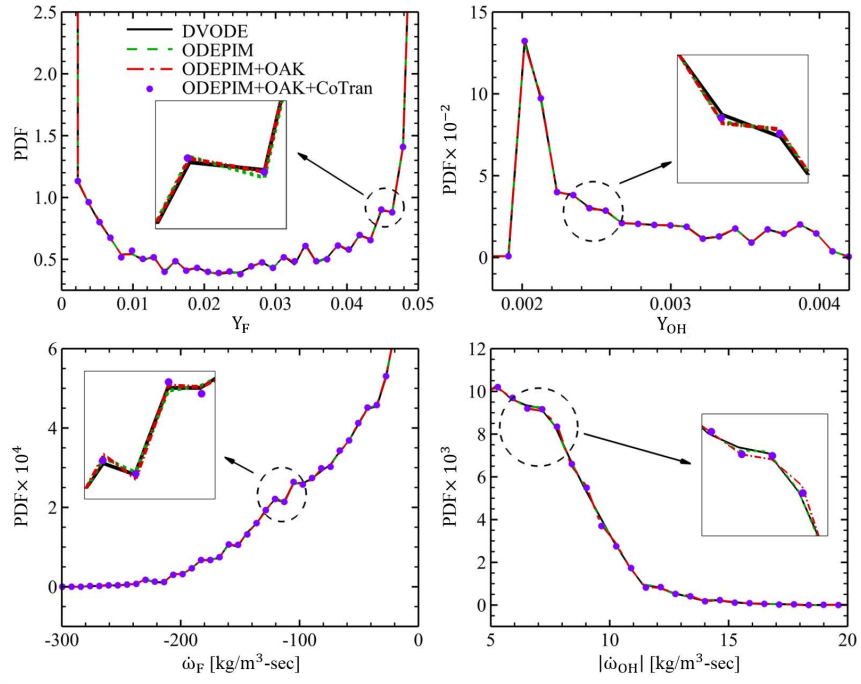

Fig. 4. PDF profiles of mass fraction (upper left) and reaction rate (lower left) of fuel, mass fraction (upper right) and absolute reaction rate (lower right) of OH.

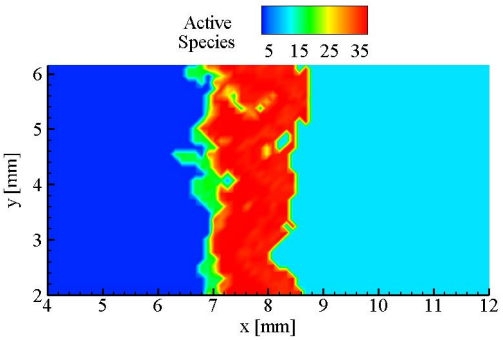

Fig. 5. Spatial distribution of the number of active species at the center plane ($z = 0.75$ cm).

with large relative errors of mass fractions and reaction rates only contain negligible corresponding values. Spatial and temporal distributions of errors are shown in Fig. S2 in the Supplemental material. Most large errors appear on the flame, and they are not sensitive to time.

3.2. Performance analysis

To understand the performance of OAK, it is necessary to visualize the correlation zones of local kinetics. Figure 5 shows the spatial distribution of active species number. Both the cold reactants side and the hot products side have small active species numbers. The cold unburnt side ($0 \leq x \leq 0.006$ m) has 2 active species (preselected fuel and O_2) and 0 active reaction. Therefore, the kinetics in the unburnt side is reduced completely. The hot side (0.009 m $\leq x \leq 0.015$ m) contains 10 active species and 27 active reactions, which is a size tolerable to conventional DNS/LES. In particular, the burnt side has more active species and reactions, due to the long lifespan of some minor species like OH. Large active species numbers only exist near the flame surface, and the buffer layers between the flame and non-flame regions have intermediate active species numbers. The brush of large kinetics is significantly wrinkled by flow turbulence.

Figure 6 shows the CPU time distribution of the four methods, to illustrate the speed-up of each component using the conventional DNS with DVODE solver as the benchmark case. The CPU time contains the OAK overhead, time for calculating chemical source terms, thermal and transport properties, and other components. With ODEPIM, calculation of the chemical source term is 17 times faster, and the total calculation is 6 times faster. With ODEPIM + OAK, the chemical source calculation is 46 times faster, but the total calculation is only 8 times faster. This is because calculation of transport properties becomes the dominant component of total CPU time when ODEPIM is applied, so significant further acceleration of chem-

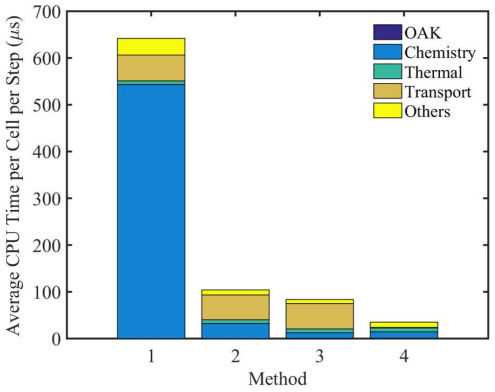

Fig. 6. Average CPU time distribution per cell per step (μs) for four methods (from left to right): DVODE, ODEPIM, ODEPIM + OAK, and ODEPIM + OAK + CoTran.

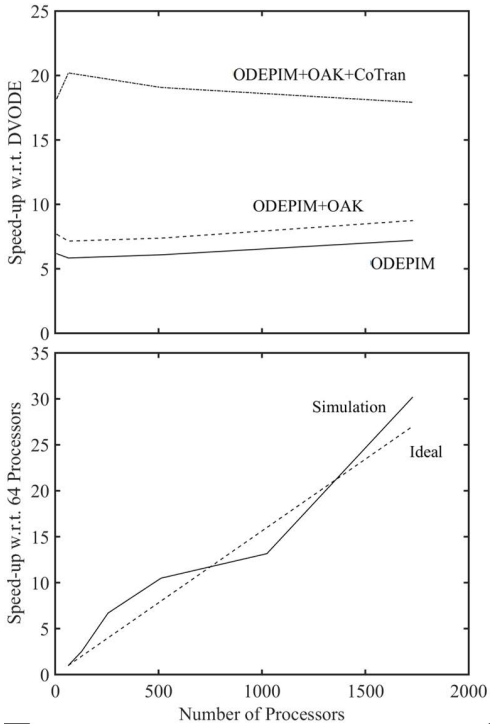

Fig. 7. Upper: weak scaling of the speed-up (w.r.t. DVODE) of the three new frameworks; lower: strong scaling of ODEPIM + OAK + CoTran.

istry calculation cannot provide a much better total speed-up. Also note that the CPU overhead of OAK is negligible, due to the space and time correlation grouping. With ODEPIM + OAK + CoTran, calculation of transport properties is 72 times faster without overhead, and the total calculation is 20 times faster. Quantified CPU time distribution can be found in Table S1 in the Supplemental material.

Full scale DNS require a large number of processors, so it is important to evaluate the parallel scalability performance of the new frameworks. Figure 7 shows the weak scaling of the speed-up for all three new frameworks, and the strong scaling of ODEPIM + OAK + CoTran. 32^3 grid cells/processor are used in weak scaling test, and the profiles of the speed-up of all three new frameworks are roughly flat, which indicates a good weak scaling of speed-up. The strong scaling test utilizes a grid of 256^3 cells ($\frac{\delta_f}{\Delta x} = 7.3$, $k_{max}\eta = 0.713$), and uses the CPU time of 64 processors as the benchmark. The strong scaling profile fluctuates slightly around the ideal curve, which indicates a good strong scaling.

4. Conclusion

A new framework for 3D DNS of turbulent combustion is developed by combining OAK, CoTran, and ODEPIM strategies. ODEPIM is a fast semi-implicit stiff ODE solver, which has accuracy similar to that of an implicit solver, and speed similar to that of an explicit solver. Simulation results show that in this test, calculation of the chemical source term is 17 times faster with ODEPIM as compared to DVODE, a pure implicit solver. OAK utilizes the PFA method to reduce the kinetic mechanism for each location and time step, which significantly reduces the stiffness of the highly nonlinear kinetic system and greatly accelerates the calculation of the chemical source term. The kinetics in the cold unburnt side is reduced to zero reaction, which indicates that OAK provides an optimized local reduction. Thermo-chemical zones are introduced and only one PFA calculation is required for each zone, which diminishes the CPU overhead of OAK to negligible. Overall, in this test, with ODEPIM + OAK, the chemical source calculation is 2.7 times faster than ODEPIM, and 46 times faster than DVODE. CoTran use a similar correlation technique to reduce the calculation of MAD transport properties, which is the dominant component of total CPU time after application of ODEPIM. In this test, calculation of the transport properties is 72 times faster, and the total calculation is 20 times faster than DVODE. A turbulent premixed flame is utilized to test both the accuracy and the performance of the new framework. Verifications, including 2D contours, streamwise spatially-averaged flame structure, PDF profiles, and quantified errors indicate that the new framework provides highly accurate results. In addition, parallel scaling tests show that the new framework has good weak scaling of speed-up and good strong scaling due to the minimization of MPI communication. In summary, the new framework provides a significant speed-up of calculation of both chemistry and transport, which enables DNS with detailed kinetics, and at the same time maintains high accuracy and good parallel scaling performance.

Acknowledgments

This work was funded by the US Federal Aviation Administration (FAA) Office of Environment and Energy as a part of ASCENT Project 28a under FAA Award number: 13-C-AJFE-GIT-009, and by NASA (Grant NNX15AU96A). Any opinions, findings, conclusions or recommendations expressed in this material are those of the authors and do not necessarily reflect the views of the FAA or other ASCENT Sponsors. Suo Yang and Wenting Sun thank Weiqi Sun and Yiguang Ju at Princeton University for inspiring discussion and detailed responses regarding technical details.

Supplementary materials

Supplementary material associated with this article can be found, in the online version, at doi:10.1016/j.proci.2016.07.021.

References

[1] R.W. Bilger, S.B. Pope, K.N.C. Bray, J.F. Driscoll, *Proc. Combust. Inst.* 30 (1) (2005) 21–42.
[2] C. Bruno, V. Sankaran, H. Kolla, J.H. Chen, *Combust. Flame* 162 (11) (2015) 4313–4330.
[3] H. Wang, K. Luo, J. Fan, *Energy Fuels* 27 (1) (2012) 549–560.
[4] A. Gruber, J.H. Chen, D. Valiev, C.K. Law, *J. Fluid Mech.* 709 (2012) 516–542.
[5] B. Yenerdag, N. Fukushima, M. Shimura, M. Tanahashi, T. Miyauchi, *Proc. Combust. Inst.* 35 (2) (2015) 1277–1285.
[6] T. Lu, C.K. Law, *Proc. Combust. Inst.* 30 (1) (2005) 1333–1341.
[7] P. Pepiot-Desjardins, H. Pitsch, *Combust. Flame* 154 (1-2) (2008) 67–81.
[8] W. Sun, Z. Chen, X. Gou, Y. Ju, *Combust. Flame* 157 (7) (2010) 1298–1307.
[9] X. Gou, Z. Chen, W. Sun, Y. Ju, *Combust. Flame* 160 (2) (2013) 225–231.
[10] Y. Liang, S.B. Pope, P. Pepiot, *Combust. Flame* 162 (2015) 3236–3253.
[11] H. Wu, Y.C. See, Q. Wang, M. Ihme, *Combust. Flame* 162 (11) (2015) 4208–4230.
[12] W. Sun, H.A. El-Asrag, Y. Ju, in: Fifty-second AIAA Aerospace Sciences Meeting, National Harbor, Maryland, 2014 AIAA 2014-0821.
[13] W. Sun, X. Gou, H.A. El-Asrag, Z. Chen, Y. Ju, *Combust. Flame* 162 (4) (2015) 1530–1539.
[14] W. Sun, Y. Ju, in: Fifty-third AIAA Aerospace Sciences Meeting, Kissimmee, Florida, 2015 AIAA 2015-1382.
[15] W.-W. Kim, S. Menon, *Combust. Sci. Technol.* 160 (1) (2000) 119–150.
[16] V. Sankaran, S. Menon, *Proc. Combust. Inst.* 30 (1) (2005) 575–582.
[17] R.W. MacCormack, *J. Spacecr. Rockets* 40 (5) (2003) 757–763.
[18] P. Brown, G. Byrne, A. Hindmarsh, *SIAM J. Sci. Comput.* 10 (8) (1989) 1038–1051.
[19] T.R. Bussing, E.M. Murman, *AIAA J.* 26 (9) (1988) 1070–1078.
[20] V.R. Katta, W.M. Roquemore, *AIAA J.* 46 (7) (2008) 1640–1650.
[21] R.J. Kee, G. Dixon-Lewis, J. Warnatz, M.E. Coltrin, J.A. Miller, H.K. Moffat, Transport: a software package for the evaluation of gas-phase, multicomponent transport properties, Chemkin Collection, 1999.
[22] C.R. Wilke, *J. Chem. Phys.* 18 (4) (1950) 517–519.
[23] T.J. Poinsot, S.K. Lele, *J. Comput. Phys.* 101 (1) (1992) 104–129.
[24] R.H. Kraichnan, *Phys. Fluids* 13 (1) (1970) 22–31.